https://doi.org/10.5194/gmd-2020-5
Preprint. Discussion started: 23 January 2020

Geoscientific Model Development
Discussions
Open Access

PERICLIMv1.0: A model deriving palaeo-air temperatures from thaw depth in past permafrost regions

Tomáš Uxa[1,2], Marek Křížek[1], and Filip Hrbáček[3]

[1]Department of Physical Geography and Geoecology, Faculty of Science, Charles University, Praha, Czech Republic
[2]Department of Geothermics, Institute of Geophysics, Czech Academy of Sciences, Praha, Czech Republic
[3]Department of Geography, Faculty of Science, Masaryk University, Brno, Czech Republic

Correspondence: Tomáš Uxa (uxa@ig.cas.cz)

Abstract. Periglacial features are among the most common relics of colder climates, which repetitively occurred throughout the Quaternary, and, as such, they are widespread archives of past conditions. Climatic controls on most periglacial features, however, remain poorly established, and thus empirical palaeo-climatic reconstructions based on them are far from reliable. This study introduces and evaluates a new simple inverse modelling scheme PERICLIMv1.0 (PERIglacial CLIMate) that aims to overcome these flaws through deriving the palaeo-air temperature characteristics coupled with the thickness of the palaeo-active layer, which can be recognized in many relict permafrost-related features. The evaluation against modern temperature records showed that the model reproduces the air temperature characteristics, such as mean annual air temperature, mean air temperature of the warmest and coldest month and of the thawing and freezing season, with a mean error of $\leq 0.5\,°C$. Besides, air thawing and freezing indices both depart on average by 6 %, whereas the length of the thawing and freezing season tends to be on average underestimated and overestimated by 10 % and 4 %, respectively. The high model success rate is promising and suggests that it could become a powerful tool for reconstructing Quaternary palaeo-environments across vast areas of mid-latitudes where relict periglacial assemblages frequently occur, but their full potential remains to be exploited.

1 Introduction

Many regions of the world host a number of relict periglacial features that have been inherited from colder periods of the Quaternary. So far, these assemblages have been used to reconstruct former climatic conditions in two basic manners. The first searches for representative analogues in terms of composition in present-day periglacial environments and associates their climates with relict features. The second assigns current climatic thresholds of active features to complex relict periglacial assemblages to deduce the most plausible palaeo-climate (Ballantyne and Harris, 1994). Such empirical interpretations, however, largely rely on flawed assumptions because suitable analogues for past periglacial environments are rare due to substantial differences in solar insolation between mid and high latitudes (Williams, 1975; French, 2017), and even if they can be found, active features present there may have developed under climatic conditions different from those which prevail at the present time (Uxa et al., 2017; Ballantyne, 2018). Climatic controls on most periglacial features are therefore poorly established, usually implying broad ranges of conditions (Washburn, 1980; Harris, 1982, 1994; Karte, 1983; Wayne, 1983; Ballantyne and Harris, 1994; Huijzer and Isarin, 1997; Ballantyne, 2018), which also relates to the fact that the features partly depend on other factors such as ground physical properties, hydrology, topography, or ground-surface cover (Ballantyne, 2018). Consequently, the inferred palaeo-climates have frequently been thought to be far from reliable, and indeed most periglacial features have been widely accepted only as indicators of seasonal frost or permafrost and ground-ice presence, but this may be dubious and rather tentative for some features as well (Ballantyne and Harris, 1994; Ballantyne, 2018). This adverse situation can largely be attributed to a persistent excessive interest in distribution patterns of periglacial features and their association with mean annual air temperature (MAAT), pervading traditional palaeo-periglacial geomorphology, while their geometric attributes have been widely neglected. Greater emphasis on the latter, closely related to the feature formation and responsible processes, could, however, advance the discipline far beyond its current frontiers (cf. Barsch, 1993; French and Thorn, 2006).

Periglacial features form through various thermally- and gravity-induced processes that mostly operate within a layer of seasonal freezing and thawing, the base of which commonly confines the subsurface dimensions of the features (Williams, 1961). The latter is usually discernible in vertical cross-sections because intense ice segregation and mass displacements associated with the feature formation alter the freeze-thaw layer so that its composition and properties differ from those of the underlying ground (French, 2017). Thus, if such an interface resides relict periglacial features, it may indicate the thickness of the palaeo-freeze-thaw layer. Since the latter closely couples with ground and air temperature conditions (e.g., Frauenfeld et al., 2004; Åkerman and Johansson, 2008; Wu and Zhang, 2010), its former level retains a valuable palaeo-climatic record that can be approximated based on modern air temperature–freeze-thaw depth relations (Williams, 1975) or can be retrieved through an inverse solution of the equations calculating the freeze-thaw depth (Maarleveld, 1976; French, 2008). Obviously, this idea is not new, but despite its simplicity and general acceptance in a benchmark periglacial literature (Washburn, 1979; Ballantyne and Harris, 1994; French, 2017; Ballantyne, 2018), it has never been developed into a viable tool for deriving past thermal regimes because computational methods have been durably underused by periglacial geomorphologists interested in reconstructions of Quaternary palaeo-environments.

This study introduces and evaluates a simple modelling scheme PERICLIMv1.0 (PERIglacial CLIMate) that is designed to infer air temperature characteristics associated with former periglacial features indicative of the base of the palaeo-active layer, and discusses its uncertainties and applicability. It specifically targets on palaeo-active-layer phenomena because their palaeo-environmental significance as well as preservation potential is substantially higher compared to seasonal-frost features. Besides, it intends to stimulate the application of modelling tools and foster the development of new quantitative methods in palaeo-environmental reconstructions exploiting relict periglacial assemblages in order to raise their reputation as palaeo-proxy indicators.

2 Model description

The PERICLIMv1.0 model principally builds on an inverse solution of the Stefan (1891) equation, which has originally been developed to determine the thickness of sea ice, but it also well describes the thaw propagation in ice-bearing grounds, and lately it has become probably the most commonly used analytical tool to estimate the thickness of the active layer (e.g., Klene et al., 2001; Shiklomanov and Nelson, 2002; Hrbáček and Uxa, 2019). It assumes that the thawed-zone temperature decreases

https://doi.org/10.5194/gmd-2020-5
Preprint. Discussion started: 23 January 2020

linearly with depth, while the bottom frozen zone is constantly at 0 °C and latent heat is the only energy sink associated with its thawing. Here, it is solved for a uniform, non-layered ground while ignoring any of its thaw-related mechanical responses.

2.1 Driving parameters

The model is driven by the thaw depth $\xi\,(\mathrm{m})$, the bulk thermal conductivity of the thawed ground k_t $(\mathrm{W\,m^{-1}\,K^{-1}})$, the volumetric ground moisture content $\phi\,(-)$, the thawing *n*-factor $n_\mathrm{t}\,(-)$, the annual amplitude of air temperature oscillations $A_\mathrm{a}\,(^\circ\mathrm{C})$ or, alternatively, the mean air temperature of the warmest month MATWM $(^\circ\mathrm{C})$, and the period of the air temperature oscillations $P\,(\mathrm{d})$ (Table 1). The ground physical parameters are assumed to characterize the entire modelling domain (∼active layer) and they are constant over time.

2.2 Ground-surface and air thawing index

The simplest scheme of the Stefan solution for calculating the thaw depth in homogeneous substratum with constant physical properties has the following form (Lunardini, 1981):

$$\xi = \sqrt{\frac{2k_\mathrm{t}I_\mathrm{ts}}{L\phi\rho_\mathrm{w}}}, \tag{1}$$

where I_ts is the ground-surface thawing index defined as a sum of positive daily ground-surface temperatures in the thawing season $(^\circ\mathrm{C\,d})$, L is the specific latent heat of fusion of water (334 000 $\mathrm{J\,kg^{-1}}$), and ρ_w is the density of water (1 000 $\mathrm{kg\,m^{-3}}$). Please note that I_ts must be multiplied by the scaling factor of 86 400 $\mathrm{s\,d^{-1}}$ in Eq. (1) to obtain the thaw depth in meters. Besides, the product of ϕ and ρ_w can be alternatively substituted by that of the gravimetric ground moisture content and the dry bulk density of the ground because their results are identical.

The ground-surface thawing index required to reach the specific thaw depth can be obtained if Eq. (1) is rearranged such as:

$$I_\mathrm{ts} = \frac{\xi^2 L\phi\rho_\mathrm{w}}{2k_\mathrm{t}}. \tag{2}$$

The ground-surface thawing index can then be converted into the air thawing index I_ta $(^\circ\mathrm{C\,d})$ through the so-called thawing *n*-factor (Lunardini, 1978), which is a simple empirical transfer function that has been widely used to parametrize the air–ground temperature relations across permafrost landscapes (e.g., Klene et al., 2001; Gisnås et al., 2017):

$$I_\mathrm{ta} = \frac{I_\mathrm{ts}}{n_\mathrm{t}}. \tag{3}$$

2.3 Air temperature characteristics

The temporal evolution of air temperature over a year $T_\mathrm{a}(t)$ (°C) can be well described by a sine wave (Fig. 1) such as:

$$T_\mathrm{a}(t) = \mathrm{MAAT} + \frac{A_\mathrm{a}}{2}\sin\left(\frac{2\pi t}{P}\right), \tag{4}$$

https://doi.org/10.5194/gmd-2020-5
Preprint. Discussion started: 23 January 2020

Table 1. List of input and output variables, their symbols and units.

Variable	Symbol	Unit
Thaw depth	ξ	m
Thawed ground thermal conductivity	k_{t}	$\mathrm{W\,m^{-1}\,K^{-1}}$
Volumetric ground moisture content	ϕ	–
Thawing n-factor	n_{t}	–
Annual air temperature amplitude	A_{a}	$^{\circ}\mathrm{C}$
Period of air temperature oscillations	P	d
Mean annual air temperature	MAAT	$^{\circ}\mathrm{C}$
Mean air temperature of the warmest month	MATWM	$^{\circ}\mathrm{C}$
Mean air temperature of the coldest month	MATCM	$^{\circ}\mathrm{C}$
Mean air temperature of the thawing season	MATTS	$^{\circ}\mathrm{C}$
Mean air temperature of the freezing season	MATFS	$^{\circ}\mathrm{C}$
Air thawing index	I_{ta}	$^{\circ}\mathrm{C\,d}$
Air freezing index	I_{fa}	$^{\circ}\mathrm{C\,d}$
Length of the thawing season	L_{t}	d
Length of the freezing season	L_{f}	d

where t is the time (d). Note that here the amplitude corresponds to the difference between MATWM and the mean air temperature of the coldest month MATCM and, as such, it must be halved in Eq. (4) and the subsequent equations in order to characterize the annual temperature variation around MAAT. Unconventionally, the range of annual air temperature oscillations can also be expressed through MATWM (cf. Williams, 1975) if its difference from MAAT is substituted for $\frac{A_{\mathrm{a}}}{2}$ in Eq. (4) and elsewhere.

The air thawing index represents the positive area under the annual air temperature curve (Fig. 1) and can be calculated by integrating Eq. (4) over the thawing season:

$$I_{\mathrm{ta}} = \int\limits_{t_1}^{t_2} T_{\mathrm{a}}(t)\,\mathrm{d}t, \tag{5}$$

with

$$t_1 = \arcsin\left(-\frac{\mathrm{MAAT}}{\frac{A_{\mathrm{a}}}{2}}\right)\frac{P}{2\pi}, \tag{6}$$

$$t_2 = \left[\pi - \arcsin\left(-\frac{\mathrm{MAAT}}{\frac{A_{\mathrm{a}}}{2}}\right)\right]\frac{P}{2\pi}, \tag{7}$$

https://doi.org/10.5194/gmd-2020-5
Preprint. Discussion started: 23 January 2020

Geoscientific Model Development
Discussions
Open Access

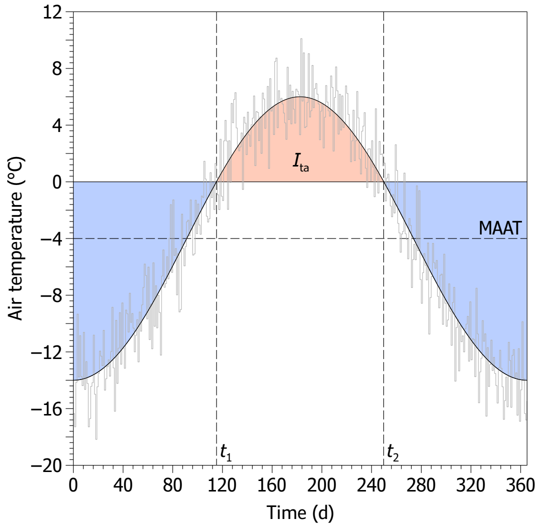

Figure 1. An idealized course of air temperature during the year expressed by a sine function with a mean of –4 °C and an amplitude of 20 °C superimposed on the annual air temperature curve with daily variations. The air thawing index is shown in red, while the blue areas depict partial air freezing indices of the preceding (left) and subsequent (right) freezing season, respectively. See text and Table 1 for abbrevations.

where t_1 is the time when the air temperature curve crosses the zero-degree Celsius level from below (∼thawing season begins), while t_2 is the time when it crosses this level from above (∼thawing season ends) (e.g., Nelson and Outcalt, 1987).

Unfortunately, Eq. (5) has no analytical solution for MAAT. The latter can be derived from a nomogram (Fig. 2), but here it is calculated numerically using the bisection root-finding method applied on the right-closed interval $(-A_\mathrm{a}, 0\rangle$. This condition ensures that both positive and negative air temperatures have occurred during the annual period, which is an essential prerequisite for the active layer to form. The same procedure can be applied in calculations based on the MATWM, but MAAT has to be searched within the interval $(-\infty, 0\rangle$ in their case because the amplitude is to be determined later. Admittedly, these assumptions are simplistic because air–ground temperatures are modulated by surface and subsurface offsets so that permafrost–seasonal frost boundary rarely coincides with MAAT of 0 °C. Instead, it usually occurs where MAAT is somewhat lower (Smith and Riseborough, 1996, 2002). However, potential drawbacks can be easily handled if exclusively permafrost-related features are examined.

Once MAAT is known, the air freezing index I_fa (°C d) can be simply computed as:

$$I_\mathrm{fa} = \mathrm{MAAT}\,P - I_\mathrm{ta} \tag{8}$$

Furthermore, MATWM and MATCM, respectively, is calculated as:

$$\mathrm{MATWM} = \mathrm{MAAT} + \frac{A_\mathrm{a}}{2}, \tag{9}$$

$$\mathrm{MATCM} = \mathrm{MAAT} - \frac{A_\mathrm{a}}{2}. \tag{10}$$

https://doi.org/10.5194/gmd-2020-5
Preprint. Discussion started: 23 January 2020

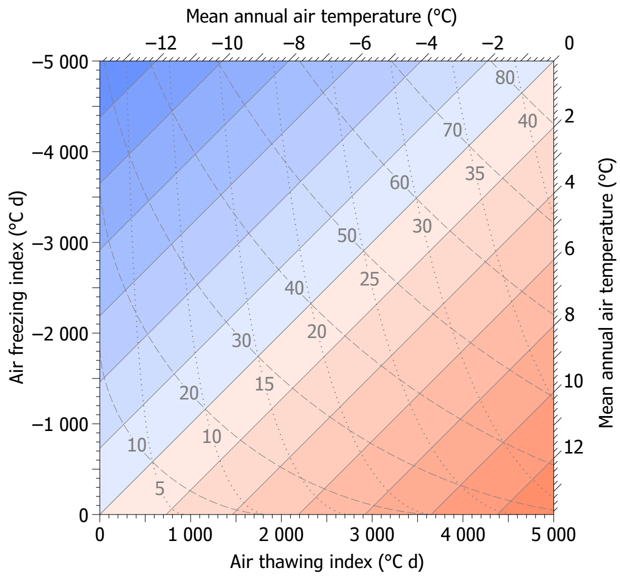

Figure 2. A nomogram showing relations between the air thawing and freezing index, mean annual air temperature (solid diagonal lines), annual air temperature amplitude (dashed curved lines), and mean air temperature of the warmest month (dotted curved lines).

Mean air temperature of the thawing MATTS (°C) and freezing MATFS (°C) season, respectively, is defined as:

$$\mathrm{MATTS} = \frac{I_{\mathrm{ta}}}{L_{\mathrm{t}}}, \tag{11}$$

$$\mathrm{MATFS} = \frac{I_{\mathrm{fa}}}{L_{\mathrm{f}}}, \tag{12}$$

where L_{t} (d) and L_{f} (d) is the duration of the thawing and freezing season, respectively, which is expressed from Eq. (6) and (7) as:

$$L_{\mathrm{t}} = t_2 - t_1 = \left[\pi - 2\arcsin\left(-\frac{\mathrm{MAAT}}{\frac{A_{\mathrm{a}}}{2}}\right)\right]\frac{P}{2\pi}, \tag{13}$$

$$L_{\mathrm{f}} = P - L_{\mathrm{t}}. \tag{14}$$

Unsurprisingly, but importantly, solutions based on alternate driving parameters, as suggested above, produce identical outcomes, allowing the model adaptations to specific situations and available data.

3 Model validation

The PERICLIMv1.0 performance was tested against mostly previously published modern temperature data obtained in the period 2009/2010 to 2017/2018 at four bare permafrost sites located on the northern, unglacierized tip of the James Ross Island, north-eastern Antarctic Peninsula, between 63°49′–63°53′ S, 57°50′–57°57′ W, and 10–340 m asl (e.g., Hrbáček et al.,

Table 2. Number of annual periods (N) along with means and ranges of the model-driving parameters at the James Ross Island (upper section) and Alaskan Arctic (lower section) validation sites.

Site	N	ξ (m)	k_{t} ($\mathrm{W\,m^{-1}\,K^{-1}}$)	ϕ (−)	n_{t} (−)	A_{a} (°C)	P (d)
Abernethly Flats	6	0.57 (0.39–0.68)	0.61	0.265	2.55 (1.60–3.21)	20.1 (17.6–21.8)	363 (350–402)
Berry Hill slopes	6	0.87 (0.85–0.90)	1.03	0.312	2.98 (2.15–4.48)	18.9 (16.0–22.2)	360 (329–403)
Johann Gregor Mendel	5	0.58 (0.51–0.65)	0.17	0.160	3.95 (2.42–6.21)	20.1 (18.4–23.0)	365 (344–403)
Johnson Mesa	6	0.58 (0.49–0.65)	0.61	0.211	3.98 (2.01–8.63)	19.4 (16.5–21.5)	360 (318–403)
Deadhorse	10	0.73 (0.68–0.78)	0.77	0.515	0.97 (0.75–1.22)	40.2 (35.9–47.5)	366 (327–422)
Franklin Bluffs	14	0.70 (0.64–0.79)	0.82	0.583	0.58 (0.43–1.24)	43.5 (40.3–49.2)	366 (350–378)
West Dock	14	0.35 (0.26–0.42)	0.60	0.725	0.49 (0.41–0.60)	37.3 (32.5–45.8)	366 (336–404)

See Table 1 for abbrevations.

2017a, b; Hrbáček and Uxa, 2019), and data collected by the Geophysical Institute Permafrost Laboratory at the University of Alaska Fairbanks in the period 2001/2002 to 2016/2017 at three vegetated permafrost locations on the coastal plain of the Alaskan Arctic adjacent to the Beaufort Sea, between 69°40′–70°22′ N, 148°28′–148°43′ W, and 3–111 m asl (https://permafrost.gi.alaska.edu/sites_list, access: 28 June 2019; Romanovsky et al., 2009; Wang et al., 2018) (Table 2). The Stefan equation has been used to calculate the active-layer thickness at some of these sites before, but with contrasting success. While on James Ross Island the thaw-depth estimates were among the most accurate ever, those from the Alaskan sites were among the worst (Romanovsky and Osterkamp, 1997; Hrbáček and Uxa, 2019). Given that both regions also differ in their climatic and environmental settings, we thus believe that they are highly suitable for PERICLIMv1.0 validation and evaluation of its limits. The stations measured air and ground temperatures with thermistor sensors installed in solar radiation shields 1.5 or 2 m above ground surface and at six to fifteen various depth levels ranging from or near from the ground surface to 0.75 m or around 1 m below, and their records were averaged to daily resolution (Romanovsky et al., 2009; Hrbáček et al., 2017a, b; Wang et al., 2018; Hrbáček and Uxa, 2019). Overall, we had 61 annual periods of data available for model validation (Table 2).

Active-layer thickness, which corresponds to the maximum annual depth of the 0 °C isotherm (Burn, 1998), was mostly determined by linear interpolation between the depths of the deepest and the shallowest sensors with the maximum annual temperature $> 0\,°\mathrm{C}$ and $\leq 0\,°\mathrm{C}$, respectively. Alternatively, it was established by linear extrapolation of the maximum annual temperatures of two deepest sensors if both were positive. The extrapolated active-layer thickness was at most 0.15 m below the deepest available temperature sensor, and thus we assume that the accuracy of the obtained values is analogous to the interpolated ones.

Thawing and freezing seasons were defined by a continued prevalence of positive and negative mean daily temperatures at the shallowest ground temperature sensor and, for consistency, these time-windows were also applied to air temperatures. Consequently, MATTS, MATFS, I_{ta}, I_{fa}, L_{t}, and L_{f} were computed. Since the model assumes that air temperatures are solely positive and negative during the thawing and freezing season, respectively (Fig. 1), positive and negative air temperatures alone

https://doi.org/10.5194/gmd-2020-5
Preprint. Discussion started: 23 January 2020

were used to determine the respective seasonal means. Likewise, MAATs were calculated as length-weighted averages of the seasonal means for periods composed of the thawing seasons and their preceding freezing seasons, which are thought to be more representative for the active-layer formation than calendar periods (Hrbáček and Uxa, 2019), but on average, they differ by only a few days from the standard length of a year at individual stations (Table 2). Annual air temperature amplitudes were defined by an annual range of a 31-day simple central moving average of mean daily air temperatures, with its extremes being considered to substitute MATWM and MATCM. Finally, thawing *n*-factors were derived as ratios of the thawing indices at the shallowest ground temperature sensors and air thawing indices. Hence, for modelling, the active-layer thicknesses had to be reduced by the depth of the shallowest ground temperature sensors in order to ensure consistency since the model presumes that the *n*-factors transfer between air and ground surface temperatures (cf. Riseborough, 2003; Hrbáček and Uxa, 2019).

Ground physical properties for the James Ross Island sites were determined in situ or from intact samples collected near the temperature monitoring stations at a depth of 0.2–0.3 m during the thawing seasons of 2013/2014, 2016/2017, and 2018/2019 (Hrbáček et al., 2017a; Hrbáček and Uxa, 2019), while those for the Alaskan sites were adapted from Zhang (1993) and Romanovsky and Osterkamp (1997) who taken samples to a depth of about 0.6 m during the thawing season of 1991 and then averaged their characteristics over the full active-layer thickness. Thawed ground thermal conductivity was determined through replicate measurements with needle thermal-conductivity probes, whereas volumetric ground moisture content was established by successive wet and dry weighing or through replicate measurements with time-domain reflectometry probes (Zhang, 1993; Hrbáček et al., 2017a; Hrbáček and Uxa, 2019). The obtained ground physical parameters (Table 2) entered the model as time-independent constants that describe the entire active-layer profile.

The model accuracy was evaluated by comparing the modelled and observed data for all sites individually and together through a simple error statistics and common error measures such as mean error (ME) and mean absolute error (MAE):

$$\mathrm{ME} = \frac{1}{N}\sum_{i=1}^{N}(m_{\mathrm{i}} - o_{\mathrm{i}}), \tag{15}$$

$$\mathrm{MAE} = \frac{1}{N}\sum_{i=1}^{N} \mid m_{\mathrm{i}} - o_{\mathrm{i}} \mid, \tag{16}$$

where m_{i} and o_{i} is the modelled and observed value, respectively, and N is the total number of model–observation pairs.

4 Results

Comparisons of the model outputs against the observed data showed that PERICLIMv1.0 reproduces the air temperature characteristics with a high accuracy at most stations, though its outcomes from James Ross Island are somewhat more precise and less scattered than those from Alaska (Fig. 3). MAAT was slightly underestimated and exhibited a site-weighted mean error and a site-weighted mean absolute error of −0.5 °C and 1 °C, respectively (Fig. 3). The absolute error was $\leq 1\,^{\circ}\mathrm{C}$ and $\leq 2\,^{\circ}\mathrm{C}$ in 57 % and 79 % of cases, respectively, and the maximum absolute error did not exceed 4.3 °C.

MATWM and MATCM evenly scattered around the identity lines and showed almost identical biases as they both attained a site-weighted mean error of −0.1 °C and a site-weighted mean absolute error of 1.1 °C (Fig. 3). Likewise, the absolute deviation

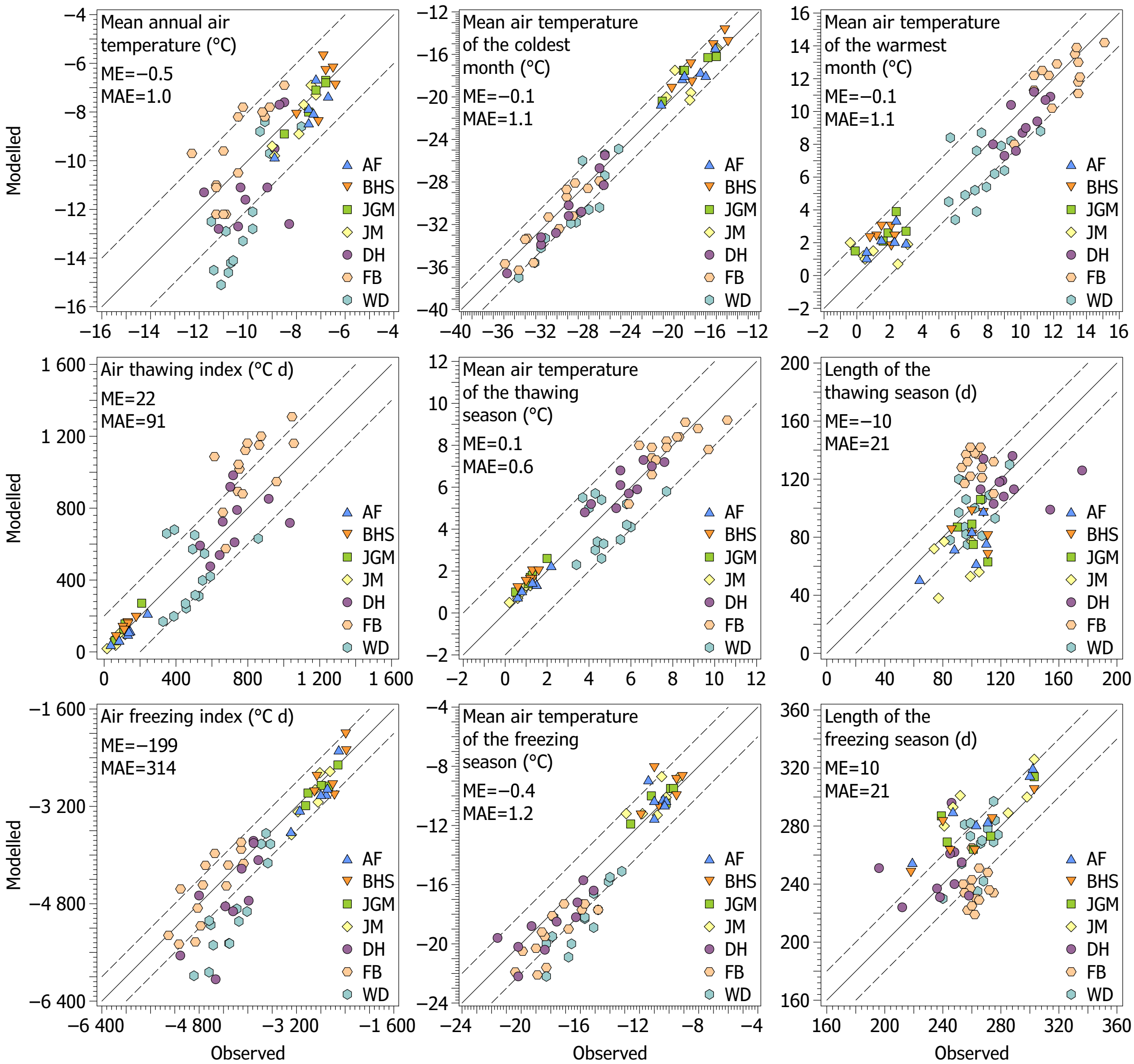

Figure 3. Observed versus modelled air temperature characteristics. Acronyms ME and MAE under the plot labels correspond to the site-weighted mean error and the site-weighted mean absolute error, respectively, while those at the bottom right of the plots indicate the station names: Abernethy Flats (AF), Berry Hill slopes (BHS), Johann Gregor Mendel (JGM), Johnson Mesa (JM), Deadhorse (DH), Franklin Bluffs (FB), and West Dock (WD).

was $\leq 1\,^{\circ}\mathrm{C}$ in 46 % of cases, in 84 % and 82 % it was $\leq 2\,^{\circ}\mathrm{C}$ for MATWM and MATCM, respectively, and the error was at worst 3.4 °C for both characteristics.

180 I_{ta} was rather uniformly distributed around the identity line, while I_{fa} tended to be slightly underestimated (Fig. 3). The indices showed a site-weighted mean error of 22 °C d and −199 °C d, respectively, which corresponds to about 6 % of the observed site-weighted mean values, and their site-weighted mean absolute error was 91 °C d and 314 °C d, respectively (Fig. 3).

I_{ta} biased by $\leq 20\,°\mathrm{C\,d}$ in 23 % of cases, and in 38 % by $\leq 40\,°\mathrm{C\,d}$. I_{fa}, which achieves one order of magnitude larger values, deviated by $\leq 200\,°\mathrm{C\,d}$ in 41 % of cases and by $\leq 400\,°\mathrm{C\,d}$ in 66 %. The maximum absolute departures of I_{ta} and I_{fa} reached 473 °C d and 1 512 °C d, respectively.

MATTS exhibited a site-weighted mean error and a site-weighted mean absolute error of 0.1 °C and 0.6 °C, respectively, while for MATFS the errors showed site-weighted means of –0.4 °C and 1.2 °C, respectively (Fig. 3). The agreement between the modelled and observed MATTS was better than or equal to 1 °C in 75 % of cases, and the maximum absolute error was 2 °C. In contrast, the bias in MATFS was $\leq 1\,°\mathrm{C}$ in 46 % of cases, $\leq 2\,°\mathrm{C}$ in 79 %, and at worst, it was 4.1 °C.

Because L_{t} and L_{f} inherently counteract, their characteristics mirror each other. The former tended to be a little underestimated by a site-weighted average of 10 d, while the latter was overestimated by the same duration (Fig. 3), which comprised 10 % and 4 % of the site-weighted mean observed L_{t} and L_{f}, respectively, and the site-weighted mean absolute errors achieved 21 d. The underestimation or overestimation was $\leq 20\,\mathrm{d}$ in 54 % of cases, $\leq 40\,\mathrm{d}$ in 85 %, and the maximum deviation did not exceed 55 d.

5 Discussion

5.1 Model uncertainties, limitations and potential adjustments

The model exhibited a high accuracy and clear trends along the identity lines for most air temperature characteristics (Fig. 3), which suggests that it is also likely to work well over a wider range of climatic conditions. The overall success rate of the model is remarkable because active-layer thickness commonly exhibits rather moderate to low correlations with annual or winter air and ground temperature parameters, but on the other hand it mostly strongly couples with summer air and ground temperature indices (e.g., Frauenfeld et al., 2004; Åkerman and Johansson, 2008; Wu and Zhang, 2010). Since PERICLIMv1.0 inherently builds on thaw depth–summer temperature relations, which it further converts into annual or winter air temperature characteristics through A_{a} or MATWM, this scheme gives rise to its high accuracy. It should be noted that it is successful despite the ground physical parameters used have certainly experienced at least slight changes since sampling or over the validation period and show vertical variations in the active layer as well (Zhang, 1993; Hrbáček et al., 2017a; Hrbáček and Uxa, 2019). Besides, the model parameterizes air temperature behaviour with a sine wave defined by annual amplitude, which simplifies the actual evolution of air temperature and completely ignores its sub-annual variations. Finally, the Stefan equation assumes stationary conditions, and thus it well represents multi-annual averages that moderate the energy imbalances introduced by natural climatic variations, but it tends to fail at capturing inter-annual transient departures from the equilibrium state (Riseborough, 2007), which are involved in the validation dataset. Some scatter in the model estimates is therefore inevitable, and may be considerable, but it is important that the averaged outputs are close to those of the observed data (Fig. 3).

The Stefan equation in its simplest form (Eq. 1) presumes that the latent heat of phase-changing ice-water is much larger than the sensible heat required to raise the ground temperature, and thus it accounts only for the former, while the latter is completely ignored. Also, it assumes that the frozen layer is at 0 °C before thaw. These simplifications cause that it tends to overestimate the thaw depth inversely proportional to the moisture content in the active layer and its temperature at the onset of

https://doi.org/10.5194/gmd-2020-5
Preprint. Discussion started: 23 January 2020

thawing (Romanovsky and Osterkamp, 1997; Kurylyk and Hayashi, 2016). A number of correction factors can overcome these flaws. However, although simple corrections exist, besides complex implicit solutions (Kurylyk and Hayashi, 2016), they all require additional inputs such as frozen thermal conductivity and thawed and frozen volumetric heat capacity or active-layer temperature at the start of its thawing. Hence, the corrections are frequently difficult to implement even in many present-day situations and definitely are much less viable for palaeo-reconstructions. Moreover, their inverse solution is not straightforward and would probably require the application of iterative techniques.

The associated uncertainties in the ground-surface thawing index estimation are likely to produce somewhat smaller errors at higher temperatures and at higher thawing *n*-factors because the derived air temperature characteristics are increasing or decreasing functions of mostly concave-down or concave-up shape, respectively, and thus are less sloped under these conditions (Fig. 4). By contrast, at higher temperatures the model estimates are much more sensitive to the choice of thawing *n*-factor and temperature amplitude (Fig. 4). These rules partly explain why the model outputs from James Ross Island are more accurate and less scattered than those from Alaska (Fig. 3). Much more, however, is this contrast due to differences in the distribution of ground physical properties within the active layer, which is rather homogeneous at the James Ross Island sites (Hrbáček et al., 2017a; Hrbáček and Uxa, 2019), but has a two-layer structure with a thick surface layer of peat at the Alaskan locations (Zhang, 1993). Overview of published data implies that the Stefan equation tends to deviate proportionally to the peat-layer thickness in the active layer (Fig. 5), which contradicts the theoretical assumptions of the Stefan equation (Romanovsky and Osterkamp, 1997; Kurylyk and Hayashi, 2016) as the presence of peat is commonly associated with high moisture contents, but it is also consistent with the present model outcomes (Fig. 3). This is probably due to complications in obtaining representative input parameters for peaty active layers because physical properties of peat extremely differ from those of any other underlying materials. Still, the model evaluation showed that it is capable of acceptable results, despite the active layer at some of the test sites is far from being saturated or is two-layer (Table 2) and permafrost there is rather cold (Hrbáček et al., 2017a, b; Wang et al., 2018).

Sometimes, stratified profiles may also be associated with relict periglacial features, which is mostly due to post-formation pedogenic or depositional processes (French, 2017). However, if they are related to the feature formation itself, the Stefan equation can be adapted to calculate the thaw depth in multi-layered grounds (e.g., Nixon and McRoberts, 1973; Kurylyk, 2015), and its inverse solution can be easily derived as well (Appendix A). On the other hand, the internal composition of most periglacial features is usually too complicated to be discretized into multiple clearly distinguishable and laterally homogeneous sub-layers. Such complex structures are advisable to be described by a homogeneous domain rather than by layered schemes since the former is less computationally demanding and requires fewer ground physical parameters but at the same time is likely to yield accurate outcomes if a representative set of driving data is provided.

It can be assumed that the model may fail in situations when substantial warming events take place after the maximum thaw depth had been reached because air or near-surface ground temperature and active-layer thickness clearly decouple during these episodes. Besides, active layer may occasionally develop even though air temperatures remain negative throughout the summer. This is characteristic for cold permafrost regions, such as Victoria Land or Dronning Maud Land, Antarctica, where bare surfaces are highly irradiated (Lacelle et al., 2016; Kotzé and Meiklejohn, 2017). Unfortunately, PERICLIMv1.0 cannot

https://doi.org/10.5194/gmd-2020-5
Preprint. Discussion started: 23 January 2020

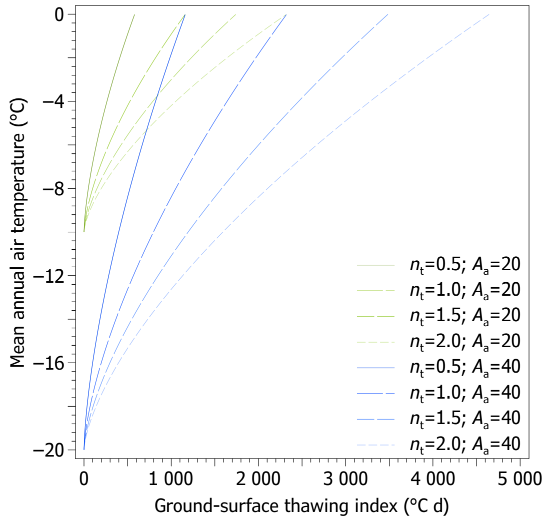

Figure 4. Modelled mean annual air temperature as a function of the ground-surface thawing index, thawing n-factor, and annual air temperature amplitude. See Table 1 for abbreviations.

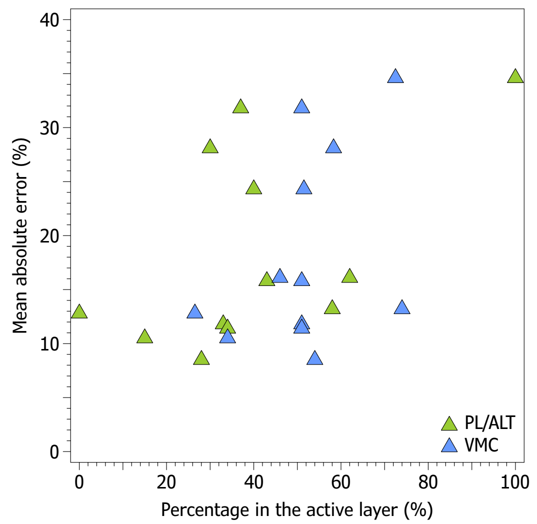

Figure 5. Mean absolute percentage error of the Stefan equation in relation to the surface peat-layer to active-layer thickness ratio (PL/ALT) and the volumetric moisture content in the active layer (VMC) based on data published in Romanovsky and Osterkamp (1997), Klene et al. (2001), and Hrbáček and Uxa (2019).

address such behaviour adequately as it assumes that MATWM is positive for both air and ground surface because n-factors cannot convert between positive and negative temperatures. Still, the model provides reasonable outputs on an annual basis if the annual air temperature oscillations are defined by A_a. By contrast, it fails completely if the annual air temperature oscillations are to be characterized by negative MATWM. Another pitfall of the MATWM-based reconstructions is their high

Geoscientific Model Development Discussions

sensitivity to variations of I_{ta} and MATWM itself (Fig. 2), which may result in major errors if the input parameters are defined inaccurately. Unfortunately, the deviations are expected to be larger at lower I_{ta} and MATWM (Fig. 2), which are typical for permafrost regions, and thus it should be highlighted that the MATWM-based solution should be employed cautiously.

If desired, the PERICLIMv1.0 can also be utilized to derive air temperature characteristics based on the seasonal frost depth. However, snow cover is an efficient insulator that, if present, alters the ground thermal regime substantially, which in turn influences the frost depth as well. Importantly, the thickness and density of snow, which are the principal controls on ground-surface–air temperature offset in winter (Smith and Riseborough, 2002), vary enormously over time and, as such, their buffering effects cannot be easily estimated via freezing n-factors. The associated uncertainty can lead to a considerable inaccuracy of the model outputs, the magnitude of which is proportional to the freezing-index value.

5.2 Driving data

It may be argued that the present exercise is impossible to replicate for relict periglacial features because of complications associated with the choice of plausible driving parameters. Undoubtedly, the ability to obtain precise forcing data from relict features is limited. At the same time, there is also little information on ground physical properties and thermal regimes of active features, which could provide a baseline for the modelling. However, any palaeo-environmental reconstruction includes some uncertainty because of many unknowns involved. Probably the best that can be done is therefore to specify a reasonable range of environmental constraints, under which the features could have developed, and then estimate the most probable palaeo-air temperature based on random-sampling methods.

5.2.1 Ground physical properties

Unfortunately, thermal conductivity is the least available ground physical parameter for most periglacial features, while ground moisture content highly varies both locally and temporally, which substantially complicates the selection of their representative values. Sometimes, however, periglacial features may be well preserved despite their considerable age, and in these situations, some of their ground physical properties can be established based on in situ observations. Bulk density, which in most mineral grounds exhibits a relatively limited range of values (Schaetzl and Thompson, 2015), can be used to estimate saturated moisture content, and then it is possible to assess the extremes, between which the moisture likely occurred. Numerous periglacial features are, moreover, composed of frost-susceptible sandy-clay-loam mixtures that are prone to compaction (Schaetzl and Thompson, 2015) and, as such, they tend to have a high bulk density, which in turn means a lower water-holding capacity and hence a reduced uncertainty in the moisture-content estimation. In addition, the moisture involved in the phase change is typically up to a few percent lower than the total moisture content as its part always remains unfrozen at freezing temperatures (Andersland and Ladanyi, 2004) and proportionally reduces the amount of latent heat required to be absorbed for thawing. The maximum moisture content may therefore be lowered correspondingly because the unfrozen moisture content alone is, by default, not included as a model input parameter. At the same time, it should be borne in mind that unfrozen moisture likely affects the thaw-depth calculations negligibly if its ratio to the total moisture content is at levels up to tens of percent (Uxa, 2017). Contemporary measurements of ground thermal conductivity would probably be misleading because it is controlled

https://doi.org/10.5194/gmd-2020-5
Preprint. Discussion started: 23 January 2020

by other ground physical parameters that may also have changed substantially. However, these correlations can be reasonably used to estimate the ground thermal conductivity through transfer functions building on such characteristics as moisture content and dry bulk density of the ground (e.g., Farouki, 1981; Zhang et al., 2018). Definitely, it is highly advisable to assume also published data for modern analogous as they may help keep the inputs within realistic limits.

Ground physical properties could also be alternatively combined into a compound edaphic term (Nelson and Outcalt, 1987, Eq. 18), which describes the entire profile by a single value given by $E = (2k_\mathrm{t}/L\phi\rho_\mathrm{w})^{1/2}$ or $E = (2k_\mathrm{t}n_\mathrm{t}/L\phi\rho_\mathrm{w})^{1/2}$. Its simplicity seems extremely advantageous for palaeo-climatic reconstructions. Besides, it is capable to suppress the intrinsic flaws of the Stefan equation. However, the edaphic parameter is currently difficult to implement as it has commonly been determined empirically based on correlations between the thaw depth and thawing index (Nelson et al., 1997; Anisimov et al., 2002; Shiklomanov and Nelson, 2002), and thus its transferability to other locations is limited. Moreover, it has not yet been established for any specific periglacial features.

5.2.2 Thawing *n*-factor

Similarly, thawing *n*-factor has also been determined for a limited number of periglacial features (e.g., Kade et al., 2006; Walker et al., 2008). However, it is principally controlled by thawing-season ground-surface characteristics alone (e.g., Westermann et al., 2015), although it may also be slightly altered by winter snow cover (Gisnås et al., 2016). Hence, it varies within a rather narrow range for specific ground-surface covers across most regions of the northern hemisphere (e.g., Lunardini, 1978; Jorgenson and Kreig, 1988; Shur and Slavin-Borovskiy, 1993; Gisnås et al., 2017), but exhibits a somewhat larger span over Antarctica (e.g., Cannone and Guglielmin, 2009; Hrbáček et al., 2017b). Because most periglacial features develop under bare to grassy surfaces, we believe that thawing *n*-factor can be reasonably estimated based on published values for analogous ground-surface covers. The values should be adopted circumspectly though due to their potential latitudinal variations (Shur and Slavin-Borovskiy, 1993) as they have commonly been reported from high-latitude locations, around or far beyond the polar circles, where seasonal cycles outweigh daily variations and, as such, the energy balance there substantially differs from that in mid-latitudes where, by contrast, relict periglacial features predominate.

5.2.3 Annual amplitude of air temperature oscillations

The initial estimate of the annual air temperature amplitude can be based on its present-day variability that may additionally be enlarged slightly. Also, it is advisable to consider available palaeo-climatic proxy-based reconstructions and model simulations, which commonly provide MATWM or MATCM, the range of which may indicate A_a. As such, these data sources could be seemingly used for standalone reconstructions because the arithmetic mean of the monthly air temperature extremes also corresponds to MAAT. The problem, however, is that they may be asynchronous with the examined periglacial features. Moreover, they usually reconstruct the palaeo-temperature in coarse temporal and/or spatial resolutions. Nonetheless, we hypothesize that A_a undergoes comparatively lower temporal and spatial changes than MAAT, and thus the proxy-based reconstructions and model simulations can be utilized to constrain the range, in which the amplitude likely fluctuated during the feature formation.

Since the PERICLIMv1.0 assumes that periglacial features develop under quasi-steady-state conditions (see Sect. 5.3), the period of the air temperature oscillations should be fixed at the standard annual period of 365 d.

5.3 Implications for palaeo-temperature reconstructions

The PERICLIMv1.0 is thought to be applied on periglacial features that may indicate former active-layer thickness, such as some types of patterned ground, large cryoturbations, some solifluction structures, frost-wedge tops, autochthonous blockfields, mountain-top detritus, active-layer detachment slides, up-frozen clasts, indurated horizons, or frost-weathering microstructures (Ballantyne and Harris, 1994; Matsuoka, 2011; Ballantyne, 2018), which dominated mid-latitude landscapes in cold-climate periods in the past. Commonly, their relics rest in places where other palaeo-indicators are rare or absent, or emerged at different times, which enhances their palaeo-environmental significance. But since most periglacial features develop on at least decadal or centennial timescales (e.g., Karte, 1983; Matsuoka, 2001; Ballantyne, 2018), inherently involving climatic variations, we hypothesize that their depth probably rather reflects the position of a transient layer where the contact between the active layer and the uppermost permafrost at the time of their formation oscillated (cf. Shur et al., 2005). Besides, the latter implies that the palaeo-active-layer thickness usually tends to appear as a dispersed rather than a sharp boundary.

Special attention must therefore be paid to avoid potential ambiguities in the identification of both the periglacial features and the palaeo-active layer. Indeed, this can be tricky because fossil features may be severely degraded. Moreover, some of them, such as small patterned-ground features, small cryoturbations, some solifluction structures, up-frozen clasts, indurated horizons, or frost-weathering microstructures, may be produced by seasonal frost, while some look-alike features may even have a non-periglacial origin (Ballantyne and Harris, 1994; Ballantyne, 2018). Nonetheless, even if identified correctly, problems may arise in places where ground-surface level has changed over time due to deposition of sediments or erosion. Moreover, highly imprecise reconstructions can probably be expected especially for features consisting of very coarse to blocky substrates such as blockfields or mountain-top detritus, in which the vertical variability of ground physical properties is extremely large (Ballantyne, 1998), and thus it is problematic to describe it by single-value parameters. On slopes, they may also provoke non-conductive heat-transfer processes, which give rise to high-magnitude short-distance variations in ground temperatures that cannot be addressed by simple heat conduction models (Wicky and Hauck, 2017).

Given the above considerations, the model should be ideally applied to co-occurring permafrost features of the same age, which may allow a more robust estimate of the range, in which the active-layer thickness and other model driving variables probably were at the time of the feature development. The most plausible values of air temperature characteristics at that time can then be assessed through random-sampling methods. Of course, it can capture only a short snapshot of the temperature history, but this is no different from a number of other palaeo-indicators, such as various glacial deposits. Moreover, if periglacial assemblages of different ages exist in a given region, they may eventually provide a more complete record of former temperatures. Undoubtedly, dating of periglacial features is still challenging, because they may have a highly complex formation history, which partly devaluates their palaeo-environmental importance. Nonetheless, this shortcoming also becomes increasingly suppressed by improved dating methods that bring more reliable chronologies (e.g., Bateman et al., 2014; Andrieux et al., 2018; Engel et al., in review).

https://doi.org/10.5194/gmd-2020-5
Preprint. Discussion started: 23 January 2020

5.4 Progress over previous attempts

Similar attempts to infer former temperature conditions have actually been made much earlier. Williams (1975) determined the palaeo-active-layer thickness of 2.0–2.3 m from the vertical extent of cryoturbation structures, and based on air temperature–thaw depth relations in present-day permafrost environments he deduced the corresponding I_{ta} of 900 °C d. Subsequently, Williams (1975) assumed MATWM of 10 °C, on the basis of which he derived MAAT of ca. −8 °C and MATCM of ca. −25 °C. This approach has been legitimately appreciated for its ingenuity, but the reconstruction itself has been subject to criticism especially for some doubtful palaeo-environmental assumptions (see Ballantyne and Harris, 1994). Its main shortcoming, however, is that it is hardly replicable as it is purely empirical. It is also unclear how MAAT of ca. −8 °C was established because the value corresponding to I_{ta} of 900 °C d and MATWM of 10 °C is ca. −5.9 °C if sine air temperature curve is assumed (Fig. 2), while MATCM equals ca. −21.8 °C. Moreover, MAAT corresponding to the alternatively determined I_{ta} of 1500 °C d and the same MATWM of 10 °C is ca. 3.5 °C, which contradicts the permafrost presence presumed by Williams (1975).

Likewise, Maarleveld (1976) derived the palaeo-frost depth of 2.5 m based on the depth of seasonal frost-cracking fissures, but he advanced further by applying the Stefan equation to estimate I_{fa} of −2230 °C d. On the other hand, he provided no other temperature characteristics, but merely suggested that the obtained I_{fa} is inconsistent with modern permafrost occurrences. Many criticisms can also be made for this approach regarding the validity of frost-cracking features as frost-depth indicators, the equality of air and ground-surface freezing index, which ignores the snow-cover effects, or vague selection of input parameters.

Yet, the two publications (Williams, 1975; Maarleveld, 1976) definitely were original and stimulating attempts, which unfortunately have never been developed further, despite being broadly cited in recognized review publications (Washburn, 1979; Ballantyne and Harris, 1994; French, 2017; Ballantyne, 2018). PERICLIMv1.0 aims to fill this gap by combining their strengths, but advances far ahead as it has a sound mathematical basis and, importantly, provides solution that itself is replicable and lacks subjectivity.

6 Conclusions

The PERICLIMv1.0 is a novel easy-to-use model that derives the palaeo-air temperature characteristics coupled with the palaeo-active-layer thickness identifiable in relict permafrost-related features. The evaluation against modern temperature records demonstrated that the model reproduces the air temperature characteristics, such as MAAT, MATWM, MATCM, MATTS or MATFS, with a mean error of as low as ≤ 0.5 °C. Besides, I_{ta} and I_{fa} both depart on average by 6 %, while L_{t} and L_{f} tends to be on average underestimated and overestimated by 10 % and 4 %, respectively. This is well above expectations and indicates that PERICLIMv1.0 is able to perform reasonably accurately if representative driving data are supplied. Yet, there is an urgent need to further test the model in various environmental settings.

Notwithstanding that, the high model success rate is definitely promising and suggests that it could become a powerful tool for reconstructing Quaternary palaeo-environments across vast areas of mid-latitudes where relict periglacial assemblages frequently occur, but their full potential remains to be exploited. It is the very first viable solution that seeks to interpret former

https://doi.org/10.5194/gmd-2020-5
Preprint. Discussion started: 23 January 2020

Geoscientific Model Development
Discussions
Open Access

periglacial features quantitatively and in a replicable and subjectivity-suppressed manner and, as such, it may provide much more plausible periglacial-based palaeo-temperature reconstructions than ever before. Hopefully, it will be a springboard for follow-up developments of more sophisticated modelling tools that will further increase the exploitability and reliability of periglacial features as palaeo-climatic proxies.

Code and data availability. The latest version of PERICLIMv1.0 is available as R package from https://github.com/tomasuxa/PERICLIMv1.0 under the GPLv3 license. The exact version of the model used to produce this paper is archived at https://doi.org/10.5281/zenodo.3600271. The validation datasets from James Ross Island are available upon request from FH (hrbacekfilip@gmail.com), whereas those from Alaskan Arctic can be retrieved from https://permafrost.gi.alaska.edu/sites_list.

Appendix A: Ground-surface and air thawing index in a two-layer ground

If two distinct ground layers are present and the base of the bottom one is supposed to indicate the thickness of the palaeo-active layer, the Stefan equation for calculating the thaw depth in two-layer ground can be applied. It has been proposed in the following form (Nixon and McRoberts, 1973; Kurylyk, 2015):

$$\xi = -Z_1 \frac{k_{\mathrm{t_2}}}{k_{\mathrm{t_1}}} + Z_1 + \sqrt{\frac{Z_1^2 k_{\mathrm{t_2}}^2}{k_{\mathrm{t_1}}^2} + \frac{2 k_{\mathrm{t_2}} I_{\mathrm{ts}}}{L \phi_2 \rho_{\mathrm{w}}} - \frac{Z_1^2 k_{\mathrm{t_2}} \phi_1}{k_{\mathrm{t_1}} \phi_2}} \tag{A1}$$

where Z_1 is the thickness of the top sub-layer (m), the physical parameters of which are subscripted by 1, while the bottom sub-layer is denoted by the subscripts 2. The ground-surface index can then be simply expressed from Eq. (A1):

$$I_{\mathrm{ts}} = \frac{\left[(\xi + Z_1 \frac{k_{\mathrm{t_2}}}{k_{\mathrm{t_1}}} - Z_1)^2 - \frac{Z_1^2 k_{\mathrm{t_2}}^2}{k_{\mathrm{t_1}}^2} + \frac{Z_1^2 k_{\mathrm{t_2}} \phi_1}{k_{\mathrm{t_1}} \phi_2} \right] L \phi_2 \rho_{\mathrm{w}}}{2 k_{\mathrm{t_2}}} \tag{A2}$$

As in Eq. (1), the product of ϕ and ρ_{w} can be substituted by that of the gravimetric moisture content and the dry bulk density of the ground, but note that the fraction on the far right of Eq. (A1) and at the corresponding place of Eq. (A2) is simplified because the density of water in its numerator and denominator is the same. Subsequent procedures to derive the air temperature characteristics are analogous to those for the one-layer solution (Eq. 3 to 14).

Author contributions. TU came up with an initial idea with feedbacks from MK, developed the model and performed its evaluation against temperature data from James Ross Island and Alaskan Arctic, which were processed by FH and TU, respectively. TU draw figures and wrote the manuscript with inputs from MK and FH. All authors reviewed and approved the final version of the paper.

Competing interests. The authors declare that they have no conflict of interest.

https://doi.org/10.5194/gmd-2020-5
Preprint. Discussion started: 23 January 2020

Geoscientific Model Development
Discussions

Acknowledgements. The PERICLIMv1.0 development and evaluation was supported by the Czech Science Foundation, project number 17-21612S. The validation datasets from James Ross Island were collected thanks to the Ministry of Education, Youth and Sports of the Czech Republic, project number LM2015078. The Geophysical Institute Permafrost Laboratory at the University of Alaska Fairbanks is acknowledged for its continuous effort in collecting temperature data across Alaska and their online dissemination.

References

Åkerman, H. J. and Johansson, M.: Thawing permafrost and thicker active layers in sub-arctic Sweden, Permafrost Periglac., 19, 279–292, https://doi.org/10.1002/ppp.626, 2008.

Andersland, O. B. and Ladanyi, B.: Frozen Ground Engineering, 2nd Edition, John Wiley & Sons, Hoboken, USA, 2004.

Andrieux, E., Bateman, M. D., and Bertran, P.: The chronology of Late Pleistocene thermal contraction cracking derived from sand wedge OSL dating in central and southern France, Global Planet. Change, 162, 84–100, https://doi.org/10.1016/j.gloplacha.2018.01.012, 2018.

Anisimov, O. A., Shiklomanov, N. I., and Nelson, F. E.: Variability of seasonal thaw depth in permafrost regions: a stochastic modeling approach, Ecol. Model., 153, 217–227, https://doi.org/10.1016/S0304-3800(02)00016-9, 2002.

Ballantyne, C. K.: Age and Significance of Mountain-Top Detritus, Permafrost Periglac., 9, 327–345, https://doi.org/10.1002/(SICI)1099-1530(199810/12)9:4<327::AID-PPP298>3.0.CO;2-9, 1998.

Ballantyne, C. K.: Periglacial Geomorphology, John Wiley & Sons, Hoboken, USA, 2018.

Ballantyne, C. K. and Harris, C.: The Periglaciation of Great Britain, Cambridge University Press, Cambridge, UK, 1994.

Barsch, D.: Periglacial geomorphology in the 21st century, Geomorphology, 7, 141–163, https://doi.org/10.1016/B978-0-444-89971-2.50011-0, 1993.

Bateman, M. D., Hitchens, S., Murton, J. B., Lee, J. R., and Gibbard, P. L.: The evolution of periglacial patterned ground in East Anglia, UK, J. Quaternary Sci., 29, 301–317, https://doi.org/10.1002/jqs.2704, 2014.

Burn, C. R.: The Active Layer: Two Contrasting Definitions, Permafrost Periglac., 9, 411–416, https://doi.org/10.1002/(SICI)1099-1530(199810/12)9:4<411::AID-PPP292>3.0.CO;2-6, 1998.

Cannone, N. and Guglielmin, M.: Influence of vegetation on the ground thermal regime in continental Antarctica, Geoderma, 151, 215–223, https://doi.org/10.1016/j.geoderma.2009.04.007, 2009.

Engel, Z., Křížek, M., Braucher, R., Uxa, T., Krause, D., AsterTeam: ^{10}Be exposure age for sorted polygons in the Sudetes Mountains, Permafrost Periglac., in review.

Farouki, O. T.: Thermal properties of soils, Monograph 81-1, U.S. Army Cold Regions Research and Engineering Laboratory, Hanover, USA, 1981.

Frauenfeld, O. W., Zhang, T., Barry, R. G., and Gilichinsky, D.: Interdecadal changes in seasonal freeze and thaw depths in Russia, J. Geophys. Res. Atmos., 109, D05101, https://doi.org/10.1029/2003JD004245, 2004.

French, H.: Recent Contributions to the Study of Past Permafrost, Permafrost Periglac., 19, 179–194, https://doi.org/10.1002/ppp.614, 2008.

French, H. M.: The Periglacial Environment, 4th Edition, John Wiley & Sons, Hoboken, USA, 2017.

French, H. and Thorn, C. E.: The changing nature of periglacial geomorphology, Geomorphologie, 12, 165–174, https://doi.org/10.4000/geomorphologie.119, 2006.

Gisnås, K., Westermann, S., Schuler, T. V., Melvold, K., and Etzelmüller, B.: Small-scale variation of snow in a regional permafrost model, The Cryosphere, 10, 1201–1215. https://doi.org/10.5194/tc-10-1201-2016, 2016.

Gisnås, K., Etzelmüller, B., Lussana, C., Hjort, J., Sannel A. B. K., Isaksen, K., Westermann, S., Kuhry, P., Christiansen, H. H., Frampton, A., and Åkerman, J.: Permafrost Map for Norway, Sweden and Finland, Permafrost Periglac., 28, 359–378, https://doi.org/10.1002/ppp.1922, 2017.

Harris, S. A.: Identification of permafrost zones using selected permafrost landforms, in: Proceedings of the 4th Canadian Permafrost Conference, Calgary, Canada, 2–6 March 1981, 49–58, 1982.

https://doi.org/10.5194/gmd-2020-5
Preprint. Discussion started: 23 January 2020

Harris, S. A.: Climatic Zonality of Periglacial Landforms in Mountain Areas, Arctic, 47, 184–192, https://doi.org/10.14430/arctic1288, 1994.

Hrbáček, F., Kňažková, M., Nývlt, D., Láska, K., Mueller, C. W., and Ondruch, J.: Active layer monitoring at CALM-S site near J.G.Mendel Station, James Ross Island, eastern Antarctic Peninsula, Sci. Total Environ., 601–602, 987–997, https://doi.org/10.1016/j.scitotenv.2017.05.266, 2017a.

Hrbáček, F., Nývlt, D., and Láska, K.: Active layer thermal dynamics at two lithologically different sites on James Ross Island, Eastern Antarctic Peninsula, Catena, 149, 592–602, https://doi.org/10.1016/j.catena.2016.06.020, 2017b.

Hrbáček, F. and Uxa, T.: The evolution of a near-surface ground thermal regime and modeled active-layer thickness on James Ross Island, Eastern Antarctic Peninsula, in 2006–2016, Permafrost Periglac., https://doi.org/10.1002/ppp.2018, 2019.

Huijzer, A. S. and Isarin, R. F. B.: The reconstruction of past climates using multi-proxy evidence: An example of the weichselian pleniglacial in northwest and central Europe. Quaternary Sci. Rev., 16, 513–533, https://doi.org/10.1016/S0277-3791(96)00080-7, 1997.

Jorgenson, M. and Kreig, R.: A model for mapping permafrost distribution based on landscape component maps and climatic variables, in: Proceedings of the 5th International Conference on Permafrost, Vol. 1, Trondheim, Norway, 2–5 August 1988, 176–182, 1988.

Kade, A., Romanovsky, V. E., and Walker, D. A.: The N-Factor of Nonsorted Circles Along a Climate Gradient in Arctic Alaska, Permafrost Periglac., 17, 279–289, https://doi.org/10.1002/ppp.563, 2006.

Karte, J.: Periglacial Phenomena and their Significance as Climatic and Edaphic Indicators, GeoJournal, 7, 329–340, https://doi.org/10.1007/BF00241455, 1983.

Klene, A. E., Nelson, F. E., Shiklomanov, N. I., and Hinkel, K. M.: The N-Factor in Natural Landscapes: Variability of Air and Soil-Surface Temperatures, Kuparuk River Basin, Alaska, USA, Arct. Antarct. Alp. Res., 33, 140–148, https://doi.org/10.2307/1552214, 2001.

Kotzé, C. and Meiklejohn, I.: Temporal variability of ground thermal regimes on the northern buttress of the Vesleskarvet nunatak, western Dronning Maud Land, Antarctica, Antarct. Sci., 29, 73–81, https://doi.org/10.1017/S095410201600047X, 2017.

Kurylyk, B. L.: Discussion of ‘A Simple Thaw-Freeze Algorithm for a Multi-Layered Soil using the Stefan Equation’ by Xie and Gough (2013), Permafrost Periglac., 26, 200–206, https://doi.org/10.1002/ppp.1834, 2015.

Kurylyk, B. L. and Hayashi, M.: Improved Stefan Equation Correction Factors to Accommodate Sensible Heat Storage during Soil Freezing or Thawing, Permafrost Periglac., 27, 189–203, https://doi.org/10.1002/ppp.1865, 2016.

Lacelle, D., Lapalme, C., Davila, A. F., Pollard, W., Marinova, M., Heldmann, J., and McKay, C. P.: Solar Radiation and Air and Ground Temperature Relations in the Cold and Hyper-Arid Quartermain Mountains, McMurdo Dry Valleys of Antarctica, Permafrost Periglac., 27, 163–176, https://doi.org/10.1002/ppp.1859, 2016.

Lunardini, V. J.: Theory of N-factors and correlation of data, in: Proceedings of the 3rd International Conference on Permafrost, Vol. 1, Edmonton, Canada, 10–13 July 1978, 40–46, 1978.

Lunardini, V. J.: Heat Transfer in Cold Climates, Van Nostrand Reinhold Co., New York, USA, 1981.

Maarleveld, G. C.: Periglacial phenomena and the mean annual temperature during the last glacial time in the Netherlands, Biul. Peryglac., 26, 57–78, 1976.

Matsuoka, N.: Solifluction rates, processes and landforms: a global review. Earth-Sci. Rev., 55, 107–134, https://doi.org/10.1016/S0012-8252(01)00057-5, 2001.

Matsuoka, N.: Climate and material controls on periglacial soil processes: Toward improving periglacial climate indicators, Quaternary Res., 75, 356–365, https://doi.org/10.1016/j.yqres.2010.12.014, 2011.

Nelson, F. E. and Outcalt, S. I.: A Computational Method for Prediction and Regionalization of Permafrost, Arctic Alpine Res., 19, 279–288, https://doi.org/10.1080/00040851.1987.12002602, 1987.

Nelson, F. E., Shiklomanov, N. I., Mueller, G. R., Hinkel, K. M., Walker, D. A., and Bockheim, J. G.: Estimating Active-Layer Thickness over a Large Region: Kuparuk River Basin, Alaska, U.S.A., Arct. Antarct. Alp. Res., 29, 367–378, https://doi.org/10.1080/00040851.1997.12003258, 1997.

Nixon, J. F. and McRoberts, E. C.: A Study of Some Factors Affecting the Thawing of Frozen Soils, Can. Geotech. J., 10, 439–452, https://doi.org/10.1139/t73-037, 1973.

Riseborough, D. W.: Thawing and freezing indices in the active layer, in: Proceedings of the 8th International Conference on Permafrost, Vol. 2, Zürich, Switzerland, 20–25 July 2003, 953–958, 2003.

Riseborough, D. W.: The Effect of Transient Conditions on an Equilibrium Permafrost-climate Model, Permafrost Periglac., 18, 21–32, https://doi.org/10.1002/ppp.579, 2007.

Romanovsky, V. E., Kholodov, A. L., Cable, W. L., Cohen, L., Panda, S., Marchenko, S., Muskett, R. R., and Nicolsky, D.: Network of Permafrost Observatories in North America and Russia, NSF Arctic Data Center, Santa Barbara, CA, USA, https://doi.org/10.18739/A2SH27, 2009.

Romanovsky, V. E. and Osterkamp, T. E.: Thawing of the Active Layer on the Coastal Plain of the Alaskan Arctic, Permafrost Periglac., 8, 1–22, https://doi.org/10.1002/(SICI)1099-1530(199701)8:1<1::AID-PPP243>3.0.CO;2-U, 1997.

Schaetzl, R. J. and Thompson, M. L.: Soil: Genesis and Geomorphology, 2nd Edition, Cambridge University Press, Cambridge, UK, 2015.

Shiklomanov, N. I. and Nelson, F. E.: Active-Layer Mapping at Regional Scales: A 13-Year Spatial Time Series for the Kuparuk Region, North-Central Alaska, Permafrost Periglac., 13, 219–230, https://doi.org/10.1002/ppp.425, 2002.

Shur, Y., Hinkel, K. M., and Nelson, F. E.: The Transient Layer: Implications for Geocryology and Climate-Change Science. Permafrost Periglac., 16, 5–17, https://doi.org/10.1002/ppp.518, 2005.

Shur, Y. L. and Slavin-Borovskiy, V. B.: N-factor maps of Russian permafrost region, in: Proceedings of the 6th International Conference on Permafrost, Vol. 1, Beijing, China, 5–9 July 1993, 564–568, 1993.

Smith, M. W. and Riseborough, D. W.: Permafrost Monitoring and Detection of Climate Change, Permafrost Periglac., 7, 301–309, https://doi.org/10.1002/(SICI)1099-1530(199610)7:4<301::AID-PPP231>3.0.CO;2-R, 1996.

Smith, M. W. and Riseborough, D. W.: Climate and the Limits of Permafrost: A Zonal Analysis, Permafrost Periglac., 13, 1–15, https://doi.org/10.1002/ppp.410, 2002.

Stefan J.: Über die Theorie der Eisbildung, insbesondere über die Eisbildung im Polarmeere. Ann. Phys., 278, 269–286, https://doi.org/10.1002/andp.18912780206, 1891.

Uxa, T.: Discussion on 'Active Layer Thickness Prediction on the Western Antarctic Peninsula' by Wilhelm et al. (2015), Permafrost Periglac., 28, 493–498, https://doi.org/10.1002/ppp.1888, 2017.

Uxa, T., Mida, P., and Křížek, M.: Effect of Climate on Morphology and Development of Sorted Circles and Polygons. Permafrost Periglac., 28, 663–674, https://doi.org/10.1002/ppp.1949, 2017.

Walker, D. A., Epstein, H. E., Romanovsky, V. E., Ping, C. L., Michaelson, G. J., Daanen, R. P., Shur, Y., Peterson, R. A., Krantz, W. B., Raynolds, M. K., Gould, W. A., Gonzalez, G., Nicolsky, D. J., Vonlanthen, C. M., Kade, A. N., Kuss, P., Kelley, A. M., Munger, C. A., Tarnocai, C. T., Matveyeva, N. V., and Daniëls, F. J. A.: Arctic patterned-ground ecosystems: A synthesis of field studies and models along a North American Arctic Transect, J. Geophys. Res. Biogeo., 113, G03S01, https://doi.org/10.1029/2007JG000504, 2008.

Wang, K., Jafarov, E., Overeem, I., Romanovsky, V., Schaefer, K., Clow, G., Urban, F., Cable, W., Piper, M., Schwalm, C., Zhang, T., Kholodov, A., Sousanes, P., Loso, M., and Hill, K.: A synthesis dataset of permafrost-affected soil thermal conditions for Alaska, USA, Earth Syst. Sci. Data, 10, 2311–2328, https://doi.org/10.5194/essd-10-2311-2018, 2018.

Washburn, A. L.: Geocryology: A Survey of Periglacial Environments, Edward Arnold, London, UK, 1979.

Washburn, A. L.: Permafrost features as evidence of climatic change. Earth-Sci. Rev., 15, 327–402, https://doi.org/10.1016/0012-8252(80)90114-2, 1980.

Wayne, W. J.: Paleoclimatic Inferences from Relict Cryogenic Features in Alpine Regions, in: Proceedings of the 4th International Conference on Permafrost, Vol. 1, Fairbanks, USA, 17–22 July 1983, 1378–1383, 1983.

Westermann, S., Elberling, B., Højlund Pedersen, S., Stendel, M., Hansen, B. U., and Liston, G. E.: Future permafrost conditions along environmental gradients in Zackenberg, Greenland, The Cryosphere, 9, 719–735, https://doi.org/10.5194/tc-9-719-2015, 2015.

Wicky, J. and Hauck, C.: Numerical modelling of convective heat transport by air flow in permafrost talus slopes, The Cryosphere, 11, 1311–1325, https://doi.org/10.5194/tc-11-1311-2017, 2017.

Williams, P. J.: Climatic Factors Controlling the Distribution of Certain Frozen Ground Phenomena. Geogr. Ann., 43, 339–347, https://doi.org/10.1080/20014422.1961.11880994, 1961.

Williams, R. B. G.: The British climate during the last glaciation: an interpretation based on periglacial phenomena, in: Ice Ages Ancient and Modern, Wright, A. E. and Moseley, F. (Eds.), Seel House, Liverpool, UK, 1975.

Wu, Q. and Zhang, T.: Changes in active layer thickness over the Qinghai-Tibetan Plateau from 1995 to 2007. J. Geophys. Res. Atmos., 115, D09107, https://doi.org/10.1029/2009JD012974, 2010.

Zhang, T.: Climate, Seasonal Snow Cover and Permafrost Temperatures in Alaska North of the Brooks Range, Ph.D. thesis, University of Alaska, Fairbanks, USA, 232 pp., 1993.

Zhang, M., Bi, J., Chen, W., Zhang, X., and Lu, J.: Evaluation of calculation models for the thermal conductivity of soils, Int. Commun. Heat Mass, 94, 14–23, https://doi.org/10.1016/j.icheatmasstransfer.2018.02.005, 2018.